

12. GALICIA MARGIN PERIDOTITES: UNDEPLETED ABYSSAL PERIDOTITES FROM THE NORTH ATLANTIC¹

Cynthia A. Evans,² Lamont-Doherty Geological Observatory, Palisades, New York
and
Jacques Girardeau, Laboratoire de Pétrologie Physique, Institut de Physique du Globe de Paris et
Université Paris VII, I.P.G., Paris, France

ABSTRACT

A ridge of peridotite was drilled off of the Galicia margin (Hole 637A) during ODP Leg 103. The ridge is located at the approximate boundary between oceanic and continental crust. This setting is of interest because the peridotite may be representative of upwelling upper mantle beneath an incipient ocean basin. The composition of the Galicia margin peridotite is compared with those of other North Atlantic peridotites.

Hole 637A ultramafic lithologies include clinopyroxene-rich spinel harzburgite and lherzolite, as well as plagioclase-bearing peridotites. Variations in mineral modal abundances and mineral compositions are observed but are not systematic. The peridotites are broadly similar in composition to other peridotites recovered from ocean basins, but the mineral compositions and abundances suggest that they are less depleted in basaltic components than other North Atlantic peridotites by about 10%. In particular, the peridotites are enriched in the magmaphilic elements Na, Al, and Ti, as compared with other abyssal peridotites. The high abundances of these elements suggest that the Hole 637A peridotites had experienced, at most, very small amounts of partial melting prior to their emplacement.

The presence of plagioclase rimming spinel in some samples suggests that the peridotite last equilibrated at about 9 kbar, near the transition between plagioclase- and spinel-peridotite stability fields. Temperatures of equilibration of the peridotite are calculated as 900°–1100°C.

The relatively undepleted composition of the peridotite indicates that it was emplaced at a shallow mantle level under a relatively cool thermal regime and cooled below solidus temperatures without having participated in any significant partial melting and basalt production. This is consistent with the emplacement of the peridotite during incipient rifting of the ocean basin, before a true spreading center was established.

INTRODUCTION

The Galicia margin, west of the Iberian coast, consists of several north-trending submarine ridges, which are interpreted as part of the faulted continental margin. These ridges are thought to be due to the attenuation and rifting of the continental crust prior to or during the opening of the Atlantic Ocean. The outermost ridge of this faulted margin, at the continental/oceanic crustal boundary, is composed of serpentinized peridotite and was first described by Boillot et al. (1980).

This ridge was drilled during Leg 103 (Hole 637A), and 35.9 m of serpentinized peridotite from a 73.6-m section was recovered. The existence of peridotite derived from the upper mantle raises the following questions: What is the nature of the peridotite? Why does it occur at the approximate boundary between oceanic and continental crust? And how was it emplaced?

Serpentinized peridotites are commonly recovered from fracture zones along slow-spreading ridges and ridge-parallel fault zones (e.g., Bonatti et al., 1974; Bonatti, 1976, 1978; Hamlyn and Bonatti, 1980; Dick and Fisher, 1984). These rocks, hereafter referred to as abyssal peridotites, are thought to be upper-mantle peridotites that were serpentinized and faulted upward and emplaced at crustal levels in these tectonically active regions. As such, abyssal peridotites give us information about the composition of the upper mantle beneath oceanic crust.

The Galicia margin peridotites recovered at Hole 637A are particularly interesting samples of abyssal peridotites because

they are not from a fracture zone at the ridge crest of a well-developed ocean basin. Rather, this outcrop of peridotite occurs at the margin of continental crust and was presumably emplaced during the rifting and opening of the North Atlantic Basin at this latitude. Therefore, the Galicia margin peridotites may be representative of the upwelling upper mantle beneath an *incipient* ocean basin. This paper examines the petrology and mineral chemistry of these rocks and compares them with other North Atlantic peridotites.

PETROGRAPHIC DESCRIPTION

The peridotites recovered from Hole 637A include serpentinized harzburgites and lherzolites that are cut by calcite veins (Fig. 1A). The peridotite is foliated and banded with relatively pyroxene-rich and -poor zones (Fig. 1B), and the relative modal abundances of minerals can change within 15–20 cm downhole. Modal mineral compositions range from samples with about 90% olivine, 8%–9% orthopyroxene, 2% clinopyroxene, and less than 0.5% chromium spinel to samples with 70%–75% olivine, 14%–18% orthopyroxene, 5%–7% clinopyroxene, and 1%–2% chromium spinel. A few bands in the peridotite contain plagioclase, generally 0.5%–1% by volume, although the most plagioclase-rich sample contains 2%–3% of the mineral (Fig. 2A). Modal abundances were calculated from point-count data (over 2000 points on a standard thin-section slide) and also on visual estimates. Serpentinized regions were counted as olivine; pseudomorphs after altered orthopyroxene are easily identified in thin section.

Rock textures and structures are somewhat obscured by serpentinization and calcite replacement and veining. However, disrupted porphyroclastic textures can be identified in most thin sections (Girardeau et al., this volume). Large, elongate porphy-

¹ Boillot, G., Winterer, E. L., et al., 1988. *Proc. ODP, Sci. Results*, 103: College Station, TX (Ocean Drilling Program).

² Present address: CA8, NASA, Johnson Space Center, Houston, TX 77058.

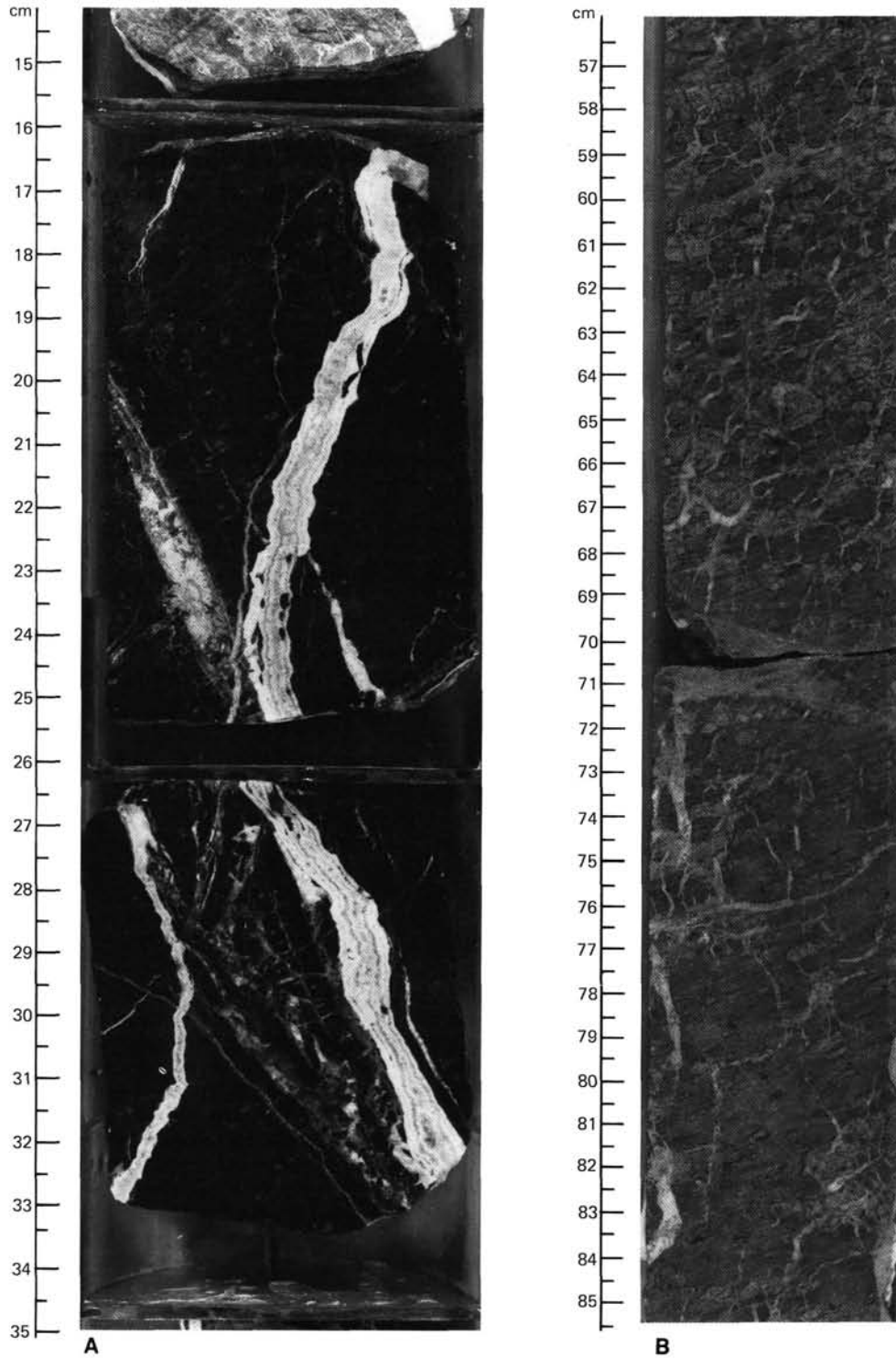


Figure 1. **A.** Sample 103-637A-27R-2, 14–35 cm. The large white, zoned vein is calcite. The “black” peridotite is relatively calcite-free. **B.** Sample 103-637A-25R-1, 56–85 cm, showing variable mineral abundances. Pyroxenes are light-colored oval spots that are aligned roughly parallel to the subhorizontal foliation. The peridotite is pyroxene-poor between 76 and 85 cm and pyroxene-rich from 56 to 70 cm.

roclasts of orthopyroxene define a foliation (Fig. 1B; Figs. 3 and 6; Girardeau et al., this volume; fig. 10 in “Site 637” chapter, Shipboard Scientific Party, 1987). Clinopyroxene grains have equant dimensions, and some grains are recrystallized. A couple of the least-altered samples display mylonitic textures, and small

(<0.1 mm) recrystallized grains of olivine, orthopyroxene, and clinopyroxene can be identified. The reader is referred to the “Site 637” chapter (Shipboard Scientific Party, 1987) and Girardeau et al. (this volume) for further discussion of rock textures and structures.

Alteration and Late-Stage Deformation

The peridotites recovered at Hole 637A are pervasively serpentinized, brecciated, and veined with calcite. Only a few samples contain relict olivine, but relict orthopyroxene and clinopyroxene are common. Downhole changes in the degree of alteration (primarily serpentinization and calcite veining) can be observed. The top of the peridotite (Cores 103-637A-23R and 103B-637A-24R) appears most leached and is completely dissected by small calcite veins and replaced by calcite (Figs. 2B and 2C). The pyroxenes appear to be particularly susceptible to calcite replacement. Some grains are completely replaced, and many grains have rims of calcite that are 0.2–0.5 mm thick. Downhole, calcite veins are ubiquitous, but minerals in the peridotite are replaced by calcite to a lesser extent.

Calcite veins, which are up to 3 cm thick and are often zoned and vugged, cut through most of the peridotite. Crosscutting relations suggest that this veining persisted to late stages of alteration of the peridotite (Fig. 1A). Oddly, some of the freshest samples (less serpentinized, without microscopic calcite veinlets or calcite replacement of mineral grains) occur adjacent to these thick calcite veins. We suggest that the large calcite veins may represent fractures in the rock that preferentially channeled fluids. The fluids would otherwise have migrated through the rock along microfractures and grain boundaries and altered the rock to a greater extent.

The relatively unaltered samples also preserve earlier high-temperature metamorphic minerals, including amphiboles (hornblends and tremolite). The amphiboles are often associated with pyroxenes but also occur in veins. In more altered samples, these mineral assemblages have retrograded to or have been overprinted by serpentine. Metamorphism and alteration of the peridotites and amphibole compositions are discussed in detail by Kimball and Evans (this volume).

Regions of the serpentinized peridotite are brecciated and probably represent fault zones. The breccia zones and veins crosscut foliation in the peridotite and some of the serpentine and calcite veins that are observed in the peridotite. Some of these fault zones are greater than 1–2 m in thickness. The peridotite around the brecciated zones is highly altered, with serpentine and calcite. The brittle deformation of both serpentine and calcite veins and the occurrence of both serpentine and calcite as matrix around breccias document several stages of serpentinization and calcite crystallization.

Mineral Composition

Mineral data from over 20 thin sections selected from the entire length of the drilled peridotite are presented. Cores of minerals were analyzed on a JEOL Superprobe 733 at Cornell University. Spot size was generally 2 μm . Pyroxene measurements were made by both broad beam and the average of several small (2 μm) spots. No compositional differences were observed between the two methods.

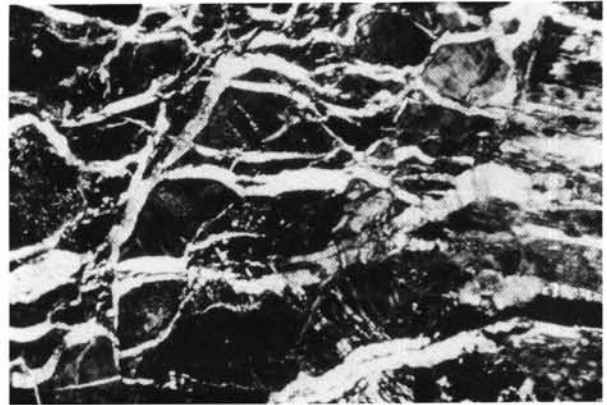
Representative compositions of the constituent minerals (olivine, orthopyroxene, clinopyroxene, chromium spinel, and plagioclase) are given in Tables 1–5. In general, mineral compositions are relatively constant and broadly similar to those from other abyssal peridotites (e.g., Dick and Fisher, 1984), although the minerals contain high concentrations of magmaphilic elements such as Na, Ti, Al, and Ca. Compositional parameters of the respective minerals are discussed in the following.

Olivine

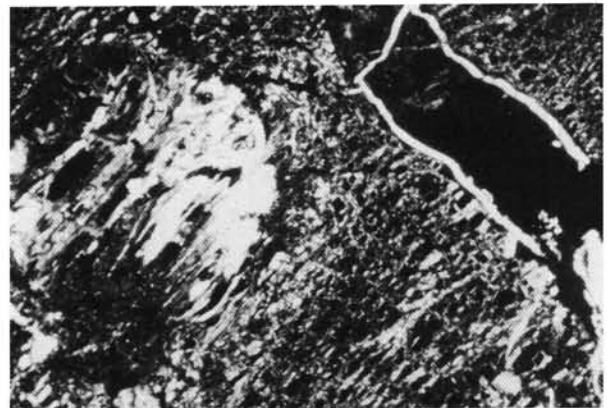
Olivine can be identified in only a few thin sections and has a very uniform composition typical of other upper mantle peridotites. Small recrystallized grains appear to have slightly more Fe-rich compositions ($\text{Fo}_{89.4-89.6}$) than larger grains, although compositions range from 89.4 to 90.6 in both sizes (Table 1).



A



B



C

Figure 2. Photomicrographs of thin sections. Scale bar is 1 mm. A. Sample 103-637A-27R-3, 33–35 cm, showing plagioclase grains rimming a chromium spinel (black grain). B. Sample 103-637A-23R-3, 65–68 cm, showing small calcite veinlets that pervasively cut through upper part of the peridotite (Cores 103-637A-23R and 103B-637A-24R). C. Sample 103-637A-24R-2, 82–85 cm. Calcite replacing clinopyroxene (round grain to left) and rimming orthopyroxene replaced by serpentine (dark grain to right).

Table 1. Representative analyses of olivine from Site 637 peridotites, with structural formulas given below. Cation abundances have been calculated per unit oxygen as indicated. All iron is treated as ferrous iron.

	103-637A-27R-3, 33-35 cm	103-637A-27R-3, 31-33 cm
SiO ₂	40.97	41.58
FeO	10.33	9.52
MnO	0.21	0.11
MgO	48.61	49.71
CaO	0.02	0.02
NiO	0.37	n.d.
	100.51	100.95
Cations/24 oxygen		
Si	6.010	6.035
Fe	1.267	1.156
Mn	0.026	0.013
Mg	10.631	10.757
Ca	0.002	0.003
Ni	0.044	
Fo	89.4	90.3

Note: n.d. = not detected.

Orthopyroxene

Orthopyroxenes have average compositions of $En_{89-90}Wo_{0.6-2.6}Fs_{8-9}$, with 3.5%–5.1% Al_2O_3 . Recrystallized grains in mylonites have low CaO, Al_2O_3 , and Cr_2O_3 contents (Table 2). Although some of the large orthopyroxene grains contain abundant exsolution lamellae, mineral compositions are remarkably constant. These compositions are plotted in Figure 3.

Clinopyroxene

Clinopyroxene grains are diopsidic with variable, but generally high, contents of Al_2O_3 (3%–7%), TiO_2 (0.1%–0.9%), Na_2O (0.45%–1.4%), and Cr_2O_3 (0.5%–1.5%) (Table 3). When plotted on the pyroxene quadrilateral (Fig. 3), pyroxene compositions demonstrate compositional uniformity, despite the differences in modal abundances of clinopyroxene in different sections and the variability in abundances of the trace elements (Na, Ti, Al, and Cr).

Positive correlations are observed between Al and Na (Figs. 4 and 5), Al and Cr (Figs. 4 and 6), and Na and Cr abundances (Figs. 4 and 7) in clinopyroxene. TiO_2 abundances do not correlate well with other compositional parameters (e.g., other magmatic elements); no correlation exists between TiO_2 and Na_2O (Fig. 8) or TiO_2 and Al_2O_3 (Fig. 9). The only noticeable trend is that the TiO_2 abundance in clinopyroxene is slightly higher in samples that contain plagioclase. Some workers (e.g., Dick and Fisher, 1984) have interpreted high TiO_2 concentrations in plagioclase peridotites to be evidence for "magmatic" clinopyroxene and plagioclase, which have crystallized from small traces of trapped mafic liquid. Textural evidence for a magmatic origin is inconclusive in the Galicia margin clinopyroxene samples.

Chromium Spinel

Light brown to red chromium spinel grains are observed in these peridotites. The spinels are aluminous ($Cr/(Cr + Al) = 0.10$ – 0.35) with respect to other abyssal peridotites (Dick and Bullen, 1984). Magnetite rims some grains, and some grains are optically and compositionally zoned with Al-rich cores and Cr- and Fe-rich rims. The compositional range observed in some individual thin sections equals the range observed from the entire

Table 2. Representative analyses of orthopyroxene from Site 637 peridotites, with structural formulas given below. Cation abundances have been calculated per unit oxygen as indicated. All iron is treated as ferrous iron.

	103-637A-23R-3, 69-70 cm (core)	103-637A-26R-4, 67-69 cm (core)	103-637A-27R-3, 31-33 cm (core)	103-637A-27R-3, 33-35 cm (recrystallized)	103-637A-27R-3 33-35 cm (rim)
SiO ₂	54.9	55.11	54.77	56.9	54.99
TiO ₂	0.01	0.1	0.18	0.17	0.21
Al ₂ O ₃	4.57	4.35	4.54	1.31	4.2
FeO	5.59	5.78	6.24	6.85	6.62
MnO	0.12	0.09	0.16	0.11	0.19
MgO	33.17	33.62	32.4	34.66	32.6
CaO	0.95	0.72	1.35	0.32	0.55
Na ₂ O ₃	0.05	0.08	0.03	0.02	0.05
K ₂ O	n.d.	0.01	0.02	n.d.	n.d.
Cr ₂ O ₃	0.8	0.67	0.59	0.21	0.62
	100.16	100.53	100.28	100.55	100.03
Cations/24 oxygen					
Si	7.566	7.571	7.569	7.828	7.609
Ti	0.001	0.01	0.018	0.017	0.022
Al	0.743	0.703	0.739	0.212	0.685
Fe	0.644	0.644	0.72	0.788	0.765
Mn	0.014	0.011	0.019	0.012	0.022
Mg	6.814	6.884	6.675	7.108	6.724
Ca	0.141	0.106	0.2	0.047	0.082
Na	0.014	0.021	0.009	0.005	0.014
K	n.d.	n.d.	0.004	n.d.	n.d.
Cr	0.087	0.072	0.064	0.022	0.067
	16.024	16.042	16.017	16.04	15.991
En	89.7	89.9	87.9	89.5	88.8
Wo	1.8	1.4	2.6	0.6	1.1
Fs	8.5	8.7	9.5	9.5	10.1

Note: n.d. = not detected.

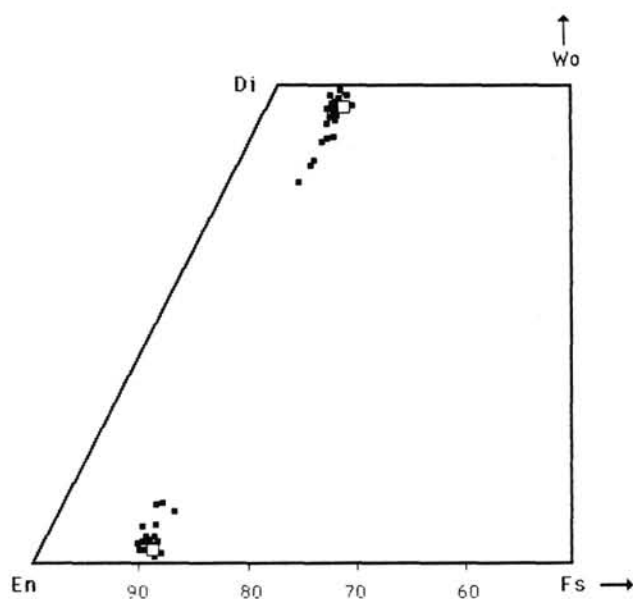


Figure 3. Pyroxene quadrilateral displaying compositions of Hole 637A pyroxenes. Open squares are pyroxene analyses from the Lers peridotite massif in the Pyrenees (C. A. Evans, unpubl. data). The pyroxene analyses are tightly clustered around $En_{89.8}Wo_{1.3}Fs_{8.9}$ (orthopyroxene) and $En_{47-49}Wo_{48-49}Fs_{3-4}$ (clinopyroxene).

peridotite section. Most of the compositional variability is attributed to alteration and is discussed by Kimball and Evans (this volume). Chromite compositions are given in Table 4 and are plotted on Figure 10.

Plagioclase

Plagioclase, where present, often rims spinel grains and occurs in pyroxene-rich bands or regions. Individual grains are up to 2–3 mm in size (Fig. 2A). Although much of the plagioclase is completely altered to saussurite, some fresh grains were identified and analyzed. Most of the plagioclase has a composition of An_{75-80} (Table 5). However, some grains adjacent to chromite show signs of strain and have been recrystallized; these grains are generally more Na-rich (An_{45-60}). Analytical difficulties (e.g., very small grain size) precluded obtaining accurate analyses from these areas.

Compositional Trends

The Site 637 peridotites from the Galicia margin represent a unique recovery of peridotite from the ocean basin in that a section of peridotite over 70 m in length was cored. To this end, lithological and compositional trends and changes resulting from alteration can be directly correlated with structures within the cores. These types of observations cannot be made from the smaller samples of abyssal peridotites recovered in dredge hauls from fracture zones.

Downhole changes in average pyroxene compositions from the peridotite are displayed in Figure 4. No downhole trends can be identified: compositional variability within a sample often equals the downhole variability between samples. However, this figure also demonstrates that certain compositional parameters covary. For example, good correlations are displayed between the Al_2O_3 abundances in orthopyroxene and clinopyroxene and the Na and Cr abundances in clinopyroxene.

Although most of the variations in mineral composition are thought to be primary, some of the downhole compositional changes are attributed to secondary processes. Certain mineral

Table 3. Representative analyses of clinopyroxene from Site 637 peridotites, with structural formulas given below. Cation abundances have been calculated per unit oxygen as indicated. All iron is treated as ferrous iron.

	103-637A-23R-3, 69–70 cm	103-637A-26R-4, 67–69 cm	103-637A-27R-3, 31–33 cm	103-637A-27R-3 33–35 cm
SiO ₂	52.52	51.99	52.01	50.81
TiO ₂	0.1	0.34	0.68	0.71
Al ₂ O ₃	4.45	6.59	4.18	6.71
FeO	1.9	2.14	2.21	2.73
MnO	0.05	0.14	0.06	0.1
MgO	15.95	15.07	16.06	15.15
CaO	22.68	21.53	22.65	21.59
Na ₂ O	0.96	1.26	0.61	0.76
K ₂ O	n.d.	n.d.	n.d.	0.02
Cr ₂ O ₃	1.31	1.5	0.96	0.98
	99.92	100.56	99.42	99.56
Cations/24 oxygen				
Si	7.627	7.49	7.597	7.409
Ti	0.001	0.036	0.074	0.077
Al	0.762	1.119	0.72	1.153
Fe	0.231	0.258	0.27	0.332
Mn	0.006	0.017	0.011	0.012
Mg	3.453	3.236	3.498	3.293
Ca	3.529	3.324	3.544	3.372
Na	0.272	0.351	0.173	0.224
K	n.d.	n.d.	n.d.	0.004
Cr	0.151	0.171	0.111	0.112
	16.032	16.002	15.998	15.998
En	47.9	47.5	47.8	47.1
Wo	48.9	48.7	48.5	48.2
Fs	3.2	3.8	3.7	4.7

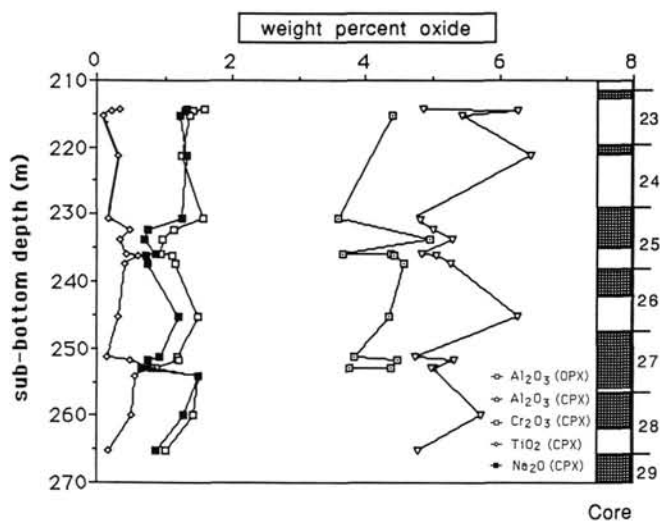


Figure 4. Downhole compositional changes (average Al, Cr, Ti, and Na abundances) in pyroxenes in the Hole 637A peridotites. Core depth is given in m sub-bottom, starting at the top of the peridotite (Core 103-637A-23R; 211.2 m sub-bottom depth). OPX = orthopyroxene; CPX = clinopyroxene.

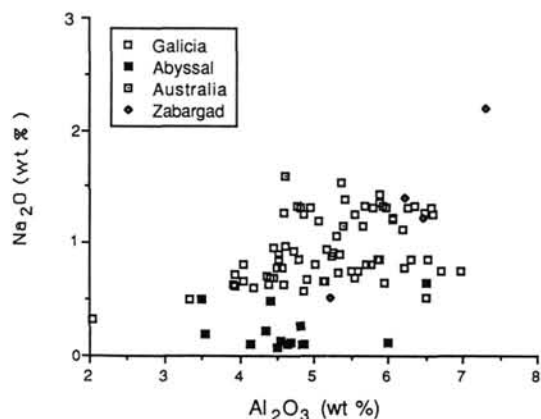


Figure 5. Al and Na abundances in clinopyroxene (CPX) from the Galicia margin peridotite, abyssal peridotites from the North Atlantic (Sinton, 1979; Prinz et al., 1976; Michael and Bonatti, 1985; Dick and Fisher, 1984), and peridotites in settings similar to the Galicia margin peridotite (southwest Australia from Nicholls, 1981; Zabargad, Red Sea, from Bonatti et al., 1986). The Galicia margin samples are enriched in Na with respect to other North Atlantic peridotites, as are the other ocean margin peridotites. All display a range of Al contents.

compositions occur in rocks with high-temperature metamorphic assemblages. For example, the formation of amphiboles can explain compositional variation in and zoning of the spinels (Al-rich cores and Cr-rich rims). Similarly, amphibole formation may account for some of the variation in Na, Al, and Ti abundances in the clinopyroxene.

DISCUSSION

Although the mineralogy and composition of the Galicia margin peridotites are generally quite similar to other peridotites recovered from ocean basins, some differences are noted. Specifically, the preceding data suggest that the Galicia margin peridotites preserve upper mantle material that is relatively undepleted in its basaltic constituents with respect to other North Atlantic peridotites. Because it is located in a unique position at the boundary between oceanic and continental crust, the Gali-

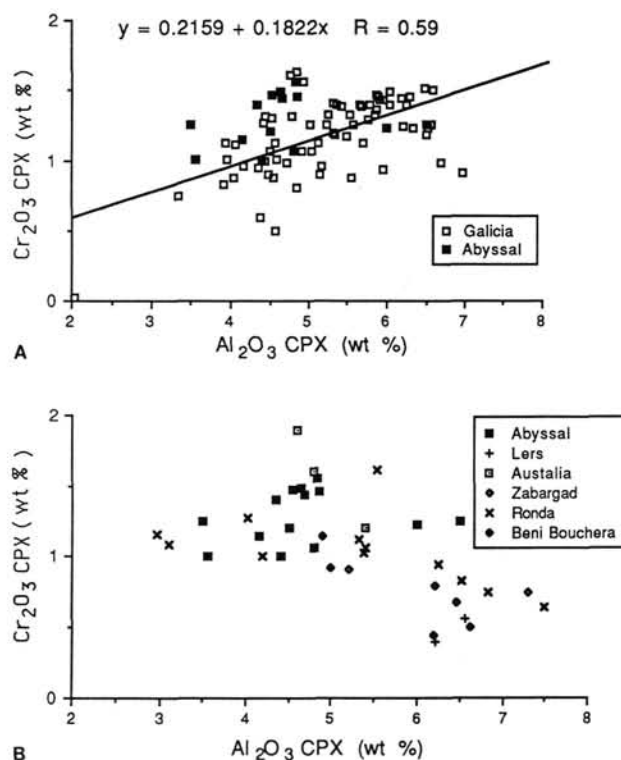


Figure 6. Al and Cr contents of clinopyroxene (CPX) from Galicia margin peridotites, abyssal peridotites from the North Atlantic, and other ocean margin peridotites. References are as in Figure 5. A positive correlation is displayed for clinopyroxene samples from Hole 637A (Fig. 6A). The linear regression is fit to the Galicia margin samples only. The field for North Atlantic abyssal peridotites is given by black symbols. Other peridotite localities in Figure 6B define a *negative* correlation between Al and Cr in clinopyroxene.

cia margin peridotite may be representative of transitional upper mantle that has not extensively participated in the production of ocean basalt.

Several authors have characterized the compositions of abyssal peridotites recovered from the ocean basins (e.g., Bonatti, 1976; Hamlyn and Bonatti, 1980; Prinz et al., 1976). Based on global compilations of abyssal peridotite compositions, Dick and Fisher (1984) and Dick and Bullen (1984) have demonstrated that the peridotites from the Atlantic Ocean Basin are more depleted in their basaltic components than those from any other ocean basin. Evidence includes the low abundance of pyroxene, the high Mg/(Mg + Fe) of olivine and orthopyroxene, and low Al₂O₃ contents in orthopyroxene, clinopyroxene, and spinel. Increases in Mg/(Mg + Fe) are correlated with decreases in pyroxene abundance and abundances of the magmaphilic elements in the rock. This is to say that North Atlantic peridotites have higher abundances of Mg, Cr, and other refractory elements and lower concentrations of Fe, Al, Ca, Na, Ti, and other magmaphilic elements.

Both Michael and Bonatti (1985) and Dick and Fisher (1984) have described regional differences in extents of depletion (using the above criteria) within the North Atlantic Basin. The compositional differences between the least and most depleted peridotites indicate a 10%–15% difference in the extent of partial melting suffered by the respective peridotites. Peridotites from the midlatitudes (35°–45°N) are the most depleted, which is attributed to the greater extent of upper mantle partial melting associated with the Azores hot spot.

In contrast, the Galicia margin peridotites are more aluminous and seemingly less refractory than other North Atlantic

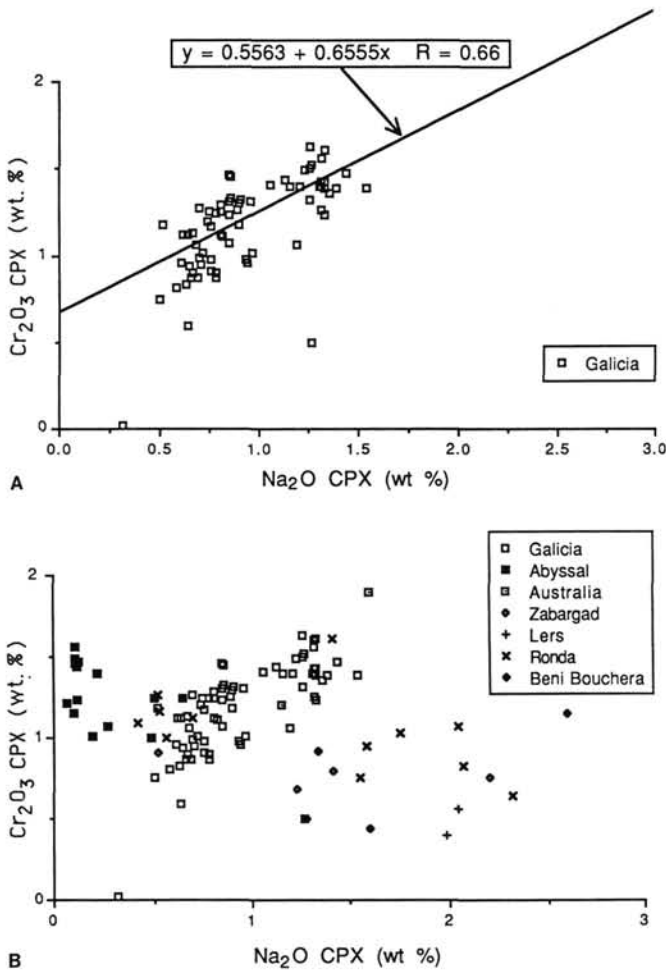


Figure 7. Na and Cr abundances in clinopyroxene (CPX). A good positive correlation is displayed between Na and Cr in the Galicia margin samples (Fig. 7A). This trend is not observed in other abyssal peridotites. Similarly, an overall negative correlation between Na and Cr is displayed by other peridotites (Fig. 7B). The two trends suggest that the Galicia margin peridotite is different from continental peridotites.

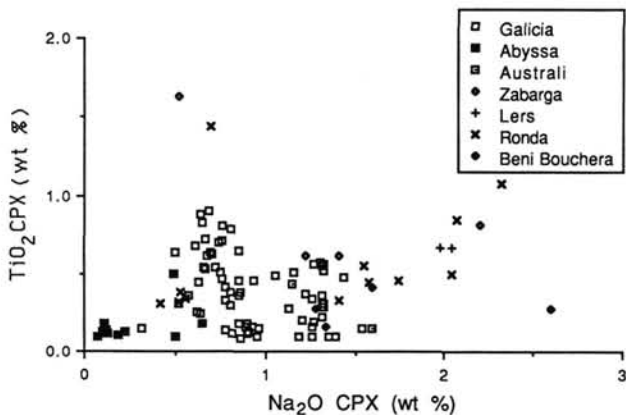


Figure 8. Na and Ti abundance in clinopyroxene (CPX). The Galicia margin peridotites have high Na abundances and a wide range of Ti abundances with respect to other abyssal peridotites. However, continental peridotites (Lers, Ronda, and Beni Bouchera) have much higher Na abundances and display a weak positive correlation between Na and Ti. The Galicia margin samples with the highest Ti are plagioclase-bearing peridotites, as are the two high-Ti points from Zabargad and Ronda.

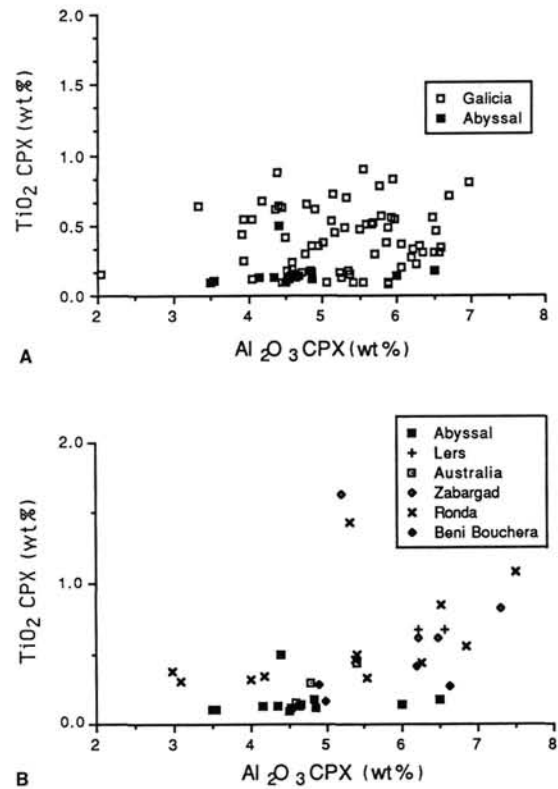


Figure 9. Al and Ti abundances in clinopyroxene (CPX). Figure 9A displays the scattered but high Ti abundances in Galicia margin clinopyroxene with respect to other North Atlantic peridotites. Figure 9B displays the coherence between Al and Ti in clinopyroxene in other peridotites. References cited are the same as those for Figure 5.

peridotites (especially those at the same latitude). Differences in compositions (%Al₂O₃ in orthopyroxene and spinel, %Na₂O and Al₂O₃ in clinopyroxene) between the Galicia margin peridotites and North Atlantic peridotites are displayed in Figures 5–10. In particular, the Galicia margin peridotite has clinopyroxene with very high Na and Al concentrations (Fig. 5) and positive correlations between Al and Cr (Fig. 6) and Na and Cr (Fig. 7). These trends are not observed in other populations of abyssal peridotites (Figs. 6 and 7). Furthermore, the spinel and orthopyroxene are more aluminous in the Galicia margin samples than in other North Atlantic peridotites (Figs. 10 and 11).

Equilibration temperatures of the peridotite were calculated using the two-pyroxene geothermometer of Bertrand and Mercier (1985). The calculations yield average temperatures of about 900°C, although the highest temperatures from the freshest rocks are 1093°C. Some of the variations in calculated temperatures can be attributed to metamorphic alteration and recrystallization: compositions from rims of grains or recrystallized grains give consistently lower calculated temperatures. Cores of pyroxenes from the freshest samples yield the highest temperatures. A more detailed discussion of geothermometry is given by Girardeau et al. (this volume). These data suggest that the peridotite was below solidus temperatures when it last equilibrated. The presence of plagioclase rims on the spinel grains indicate that this equilibration was less than 9 kbar, within the plagioclase stability field (Green and Hibberson, 1970).

Estimates of Partial Melting

Some simple modeling has been done to determine the extent of depletion of the Galicia margin peridotites with respect to other North Atlantic abyssal peridotites. The different ap-

Table 4. Representative analyses of spinel from Site 637 peridotites, with structural formulas given below. Cation abundances have been calculated per unit oxygen as indicated. All iron is treated as ferrous iron.

	103-637A-23R-3, 69–70 cm	103-637A-26R-4, 67–69 cm (core) (rim)	103-637A-27R-3, 31–33 cm (core) (rim)	103-637A-27R-3, 33–35 cm		
TiO ₂	0.02	0.04	0.05	0.16	0.2	0.17
Al ₂ O ₃	51.33	48.96	45.0	56.25	47.79	51.13
FeO	12.1	12.24	12.32	11.36	13.96	12.98
MnO	0.15	0.13	0.08	0.18	0.23	0.13
MgO	18.47	19.54	18.69	19.87	18.06	18.25
CaO	n.d.	n.d.	n.d.	n.d.	0.01	0.02
Cr ₂ O ₃	0.01					
	18.27	18.77	21.94	11.78	20.15	17.55
	100.35	99.68	98.08	99.6	100.4	100.25
Cations/32 oxygen						
Ti	0.003	0.007	0.009	0.025	0.032	0.027
Al	12.885	12.446	11.796	13.87	12.222	13.023
Fe	2.155	2.208	2.291	1.987	2.533	2.317
Mn	0.027	0.024	0.016	0.032	0.042	0.023
Mg	5.865	6.283	6.195	6.199	5.841	5.809
Ca	0.001	n.d.	n.d.	n.d.	0.002	0.004
Cr	3.077	3.201	3.858	1.948	3.456	2.962
	24.017	24.169	24.164	24.06	24.128	24.171
Cr/(Cr + Al)	0.19	0.2	0.25	0.12	0.22	0.19
Mg/(Mg + Fe)	0.37	0.74	0.73	0.76	0.7	0.72

Note: n.d. = not detected.

proaches used to estimate extent of depletion in the Hole 637A peridotites are discussed in the following. The bulk peridotite compositions that were used are given in Table 6. For reference, all of the estimates of percent melting and depletion have been made relative to the "pyrolite" composition of Green et al. (1979).

The relative extents of partial melting and subsequent depletion for these peridotites can be only crudely estimated for several reasons.

1. The peridotites exhibit a substantial range in modal abundances of minerals, which occurs on scales of centimeters to meters. Thus, bulk rock compositions are difficult to estimate.

2. The estimated composition of a hypothetical "undepleted" upper mantle peridotite is poorly constrained. This is particularly true for the abundances of trace elements such as Na and Ti. Several different estimates for compositions of pyrolite and average undepleted peridotites from nodules have been made (e.g., Green et al., 1979; Jaques and Green, 1980; Ringwood, 1979; Jagoutz et al., 1979).

3. Data on distribution coefficients for most elements in mantle phases are unavailable.

Experimental Considerations

The experimental works of Mysen and Kushiro (1977) and Jaques and Green (1980) have shown that mineral compositions in peridotite change with increasing extents of partial melting. The compositional changes displayed include overall decreases (bulk-rock and mineral compositions) in Na, Ti, Al, Ca, and Fe and increases in Mg/(Mg + Fe) and Cr/(Cr + Al), with increased partial melting of a peridotite. These compositional changes correlate with decreasing abundances of clinopyroxene as melting proceeds.

More specifically, the experimental studies of Jaques and Green (1980) on the Tinaquillo peridotite display the following: the Cr/(Cr + Al) of the chromite increases from approximately 0.22 at 10% melt to 0.50 at 15% melt. The Al₂O₃ of the ortho-

pyroxene drops from 4 wt% at 10% melt to about 2.2 wt% at 20% melt. Additional experimental data from Mysen and Kushiro (1977) indicate that Cr/(Cr + Al) = 0.2–0.3 in chromite would correspond to 2%–10% melt. Furthermore, the variation in 100 Na/(Na + Ca) of the clinopyroxene decreases from 10 to 4.5 with 0% to 15% melt.

These data suggest that compositional parameters like Al abundance in orthopyroxene, Mg/(Mg + Fe) of olivine and orthopyroxene, Cr/(Cr + Al) ratio of spinel, and Na, Ti, and Al abundances in clinopyroxene can be used to estimate relative extents of partial melting and subsequent depletion in peridotites. Exact percentages of partial melting cannot be estimated because peridotite starting compositions and the pressure and temperature of melting are unknown, and mineral compositions in the peridotite may have been effected by metamorphic recrystallization or metasomatism (e.g., Al₂O₃ in orthopyroxene, Cr/(Cr + Al) in spinel). However, the aluminous mineral compositions in the Galicia margin peridotites are consistent with estimates that they have suffered 10% or less depletion of basaltic constituents. Olivine and orthopyroxene are relatively Fe-rich, with Mg/(Mg + Fe) = 89–90 and 89–91, respectively. Pyroxenes and spinel are Al rich: orthopyroxene and clinopyroxene have Al₂O₃ concentrations as high as 4.6% and 7%, respectively, and Cr/(Cr + Al) of the chromium spinel is low (0.10–0.25) for abyssal peridotites (Fig. 10). The clinopyroxene has high Na and Ti contents (Fig. 8) and high values (between 6–10) for 100 Na/(Na + Ca).

For comparison between Galicia margin peridotites and other abyssal peridotites from the Atlantic Ocean Basin, a "high-Al" peridotite described by Dick and Fisher (1984) has orthopyroxene with 5% Al₂O₃, Mg/(Mg + Fe) = 0.903, and Cr/(Cr + Al) of spinel = 0.20. A "low-Al" peridotite (from the Mid-Atlantic Ridge) has orthopyroxene with 2.38% Al₂O₃, Mg/(Mg + Fe) = 0.914, and Cr/(Cr + Al) of spinel = 0.530. The range of compositions documented by Dick and Fisher (1984) in North Atlantic peridotites includes orthopyroxene with 4.5%–2% Al₂O₃, spinel with Cr = 0.2–0.5, and clinopyroxene with 100 Na/(Na + Ca) < 1.7.

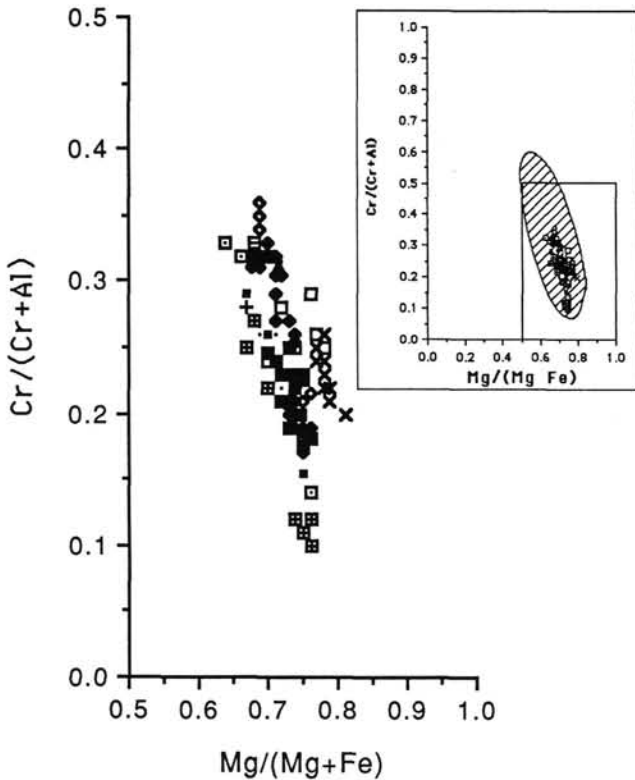


Figure 10. Mg/(Mg + Fe) vs. Cr/(Cr + Al) for spinel from Galicia margin peridotites. Each plotted point represents a thin-section sample. Shaded field is field for abyssal peridotites from Dick and Bullen (1984). The range of compositions within a thin section is close to the range displayed by the entire peridotite section. Compositional range is due to alteration of spinel.

Table 7 outlines some of the compositional changes in peridotites documented by experimental data and mineral compositions observed in the Galicia margin and North Atlantic peridotites.

Phase Diagrams

Compositions of peridotites are plotted on the Ol-An-Q phase diagram projection from Di (Fig. 12, after Presnall et al., 1979), and relative extents of partial melting from the 9.3- and 11-kbar solidus points were estimated. From the 9.3-kbar point, the Galicia margin peridotite is depleted by about 10% from pyrolite. For comparative purposes, the "more refractory" North Atlantic peridotite of Michael and Bonatti (1985) and the "average abyssal" peridotite of Dick and Fisher (1984) are about 17% and 15% more depleted than pyrolite, respectively. If melting occurred at 11 kbar, the Galicia margin peridotite would be about 11% depleted with respect to pyrolite, the average abyssal peridotite about 15.6% depleted, and the more refractory peridotite about 18% depleted.

FeO-MgO Abundances

Increasing depletion by partial melting of a peridotite results in decreasing FeO and increasing MgO abundances. It is possible to model changing FeO and MgO contents of a peridotite with increased melting. Conversely, if FeO and MgO of a peridotite are known, it is possible to make estimates of relative extents of partial melting. Using the model presented by Hanson and Langmuir (1978), which assumes batch-melting conditions, degrees of partial melting are estimated from the FeO and MgO contents of the Galicia margin peridotite (Hole 637A) and sev-

Table 5. Representative analysis of plagioclase from Site 637 peridotites, with structural formulas are given below. Cation abundances have been calculated per unit oxygen as indicated. All iron is treated as ferrous iron.

	103-637A-27R-3, 33-35 cm	103-637A-27R-3, 32-33 cm
Al ₂ O ₃	33.79	31.77
FeO	0.05	0.12
MnO	0.04	0.01
CaO	16.58	14.86
Na ₂ O	2.08	2.93
K ₂ O	n.d.	n.d.
	101.05	100.09
Cations/8 oxygen		
Si	2.197	2.293
Al	1.804	1.703
Fe	0.002	0.005
Mn	0.001	
Ca	0.805	0.724
Na	0.183	0.259
K	n.d.	n.d.
	4.992	4.984
An	81.5	73.7
Ab	18.5	26.3

Note: n.d. = not detected.

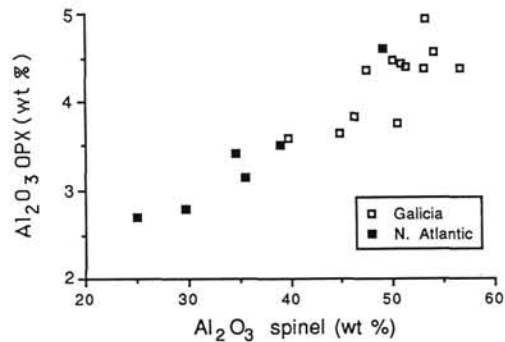


Figure 11. Al₂O₃ of orthopyroxene (OPX) vs. Al₂O₃ in coexisting chrome spinel. A weak positive correlation is displayed, but Galicia margin samples are more aluminous than other peridotites from the Atlantic basin. Comparative data are from Sinton (1979), Prinz et al. (1976), and Dick and Fisher (1984).

eral other peridotites. This model is graphically displayed in Figure 13. The relative FeO and MgO abundances of the respective peridotites indicate that the Galicia margin peridotite is depleted from pyrolite by about 10%; the Tinaquillo peridotite by about 7%-8%; the average abyssal peridotite of Dick and Fisher (1984) by 18%; less and more refractory North Atlantic peridotites of Michael and Bonatti (1985) by 11%-12% and 24%, respectively; and a North Atlantic peridotite from Prinz et al. (1976) by 20% (Fig. 13).

Models of Batch Melting

Finally, estimates of extents of partial melting experienced by the Galicia margin peridotite have been made by calculating batch-melting paths for a variety of trace elements (Na, Ti, Al, and Ca) in the peridotite. The following equations describe the distribution of trace elements during partial melting (e.g., Gast, 1968). Concentrations were recalculated to mole percent (mol%).

Table 6. Estimated bulk composition of abyssal peridotites taken from the literature.

	Hole 637A	Abyssal ^a	AT33A ^b	North Atlantic ^c	North Atlantic ^d	Tinaquillo ^e	Zabargad ^f	Pyrolite ^g
SiO ₂	44.13	43.60	44.04	44.64	43.64	44.95	45.65	45.20
TiO ₂	0.07	0.02	0.03	0.03	0.01	0.08	0.15	0.17
Al ₂ O ₃	2.31	1.18	2.01	2.2	0.65	3.22	3.85	4.40
FeO	8.81	8.20	7.41	8.27	7.83	7.65	8.44	7.60
MnO	0.19	0.14	0.05	n.d.	n.d.	0.14	0.14	0.14
MgO	42.35	45.20	44.26	42.38	46.36	40.03	38.00	38.80
CaO	2.00	1.13	0.58	0.05	0.05	3.0	3.18	3.40
Na ₂ O	0.11	0.02	0.18	0.005	0.005	0.18	0.34	0.40
K ₂ O	0.003	n.d.	0.02	0.003	0.002	0.02	0.03	0.003
Cr ₂ O ₃	0.44	n.d.	0.45	n.d.	n.d.	0.5	n.d.	0.26

^a Average abyssal peridotite, Dick and Fisher (1984).^b North Atlantic peridotite, Prinz et al. (1976).^c Less refractory North Atlantic peridotites, Michael and Bonatti (1985).^d More refractory North Atlantic peridotites, Michael and Bonatti (1985).^e Tinaquillo peridotite, Jaques and Green (1980).^f Bonatti et al. (1986).^g Pyrolite, Green et al. (1979).**Table 7. Compositional parameters for minerals in peridotites from Site 637 and the North Atlantic compared with data from partial-melting experiments (Mysen and Kushiro, 1977; Jaques and Green, 1980).**

	Mysen and Kushiro (1977)	Jaques and Green (1980)	Hole 637A	North Atlantic ^a
Orthopyroxene % melt	0%–10% (20 kbar)	10%–20% (15 kbar)		
Mg/(Mg + Fe)	0.90–0.935	0.91–0.92	0.90–0.91	0.91
Al ₂ O ₃	3.3%–2.3%	4.5%–2.5%	4.7%–>4%	3.5%–2.0%
Clinopyroxene 100 Na/(Na + Ca)	10–6		10–6 (average = 9)	1.7
Spinel % melt	0%–30%	10%–15%		
Cr/(Cr + Al)	0.20–0.30	0.25–0.50	0.10–0.25	0.35–0.53

^a Dick and Fisher (1984) and Sinton (1978).

$$C_O + FC_L + (1 + F)C_S, \quad (1)$$

where

- C_O = concentration of element in initial solid,
 C_L = concentration of the element in the liquid,
 C_S = concentration of the element in the final solid,
 F = fraction of melt, and
 D = bulk distribution coefficient = C_S/C_L .

Rearranging equation (1):

$$F = D(C_O/C_S - 1)/(1 - D). \quad (2)$$

Initial concentrations (C_O) for particular elements in an unmelted, undepleted peridotite (pyrolite) are taken from Green et al. (1979) and are given in Table 6. Final concentrations (bulk-rock concentrations) for these elements in several depleted peridotites are also given in Table 6. The bulk distribution coefficients used are based on estimated values from the literature (Dick and Bullen, 1984; Green et al., 1979; Irving, 1978) as follows:

$$D_{Na} = 0.02 \quad D_{Ti} = 0.05 \quad D_{Al} = 0.083 \quad D_{Ca} = 0.085$$

The batch-melting calculations for Na, Ti, Al, and Ca indicate that the Tinaquillo peridotite is 3%–6% depleted with respect to pyrolite (or has been partially melted by 3%–6%), the Galicia margin peridotite is 5%–9% depleted, the average abyssal

peridotite of Dick and Fisher (1984) is about 20%–40% depleted, and a North Atlantic peridotite from Prinz et al. (1976) gives variable estimates of extent of depletion. These calculations are summarized in Table 8.

These modeling results are composition and model dependent, particularly with respect to the initial composition of pyrolite. The trace element (Na, Ti, Ca, and Al) abundances in pyrolite, the Galicia margin peridotites, and other abyssal peridotites are poorly determined and may be off by factors of 2–10, depending on how the bulk compositions are constructed. The large range of results for the North Atlantic peridotites is probably due to such errors in bulk-rock compositions. These results are also very dependent on the bulk distribution coefficients (D) for each element, which, in turn, depend on similarly poorly known distribution coefficients (K_d) for individual mineral phases.

The estimated percent melt from Ti abundance is the most inconsistent. As already discussed, the TiO₂ abundance in clinopyroxene is much more variable and its behavior much less predictable than other basaltic elements (e.g., Na, Al) and appears to correspond to both the presence of plagioclase and amphibole formation. However, the petrologic reasons for the complex behavior of Ti are not clear. Therefore, TiO₂ abundance is not a reliable parameter to use for estimations of extent of depletion.

To summarize the modeling results, relative extents of partial melting and depletion have been calculated assuming batch-melting conditions, original peridotite composition, and bulk

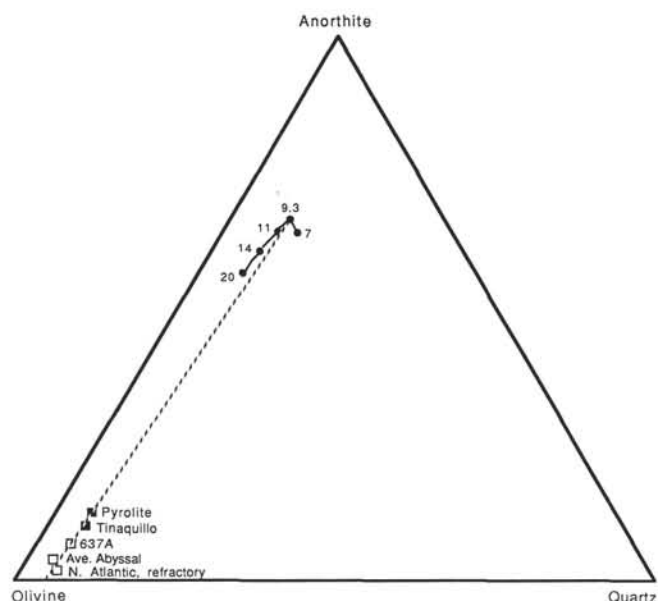


Figure 12. Anorthite-olivine-SiO₂ diagram as projected from the diopside apex after Presnall et al. (1979). Line indicates solidus invariant points for a variety of pressures (in kbar). This diagram allows relative extents of depletion to be estimated, as discussed in text. The line from the 9.3-kbar point away from pyrolite indicates the compositional path of the peridotite residuum with progressive melting.

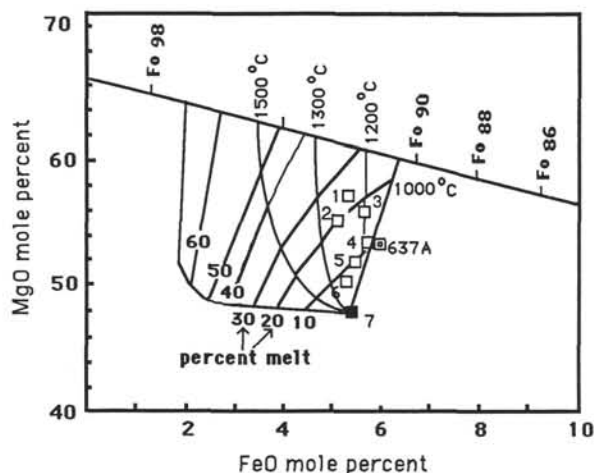


Figure 13. Relative FeO and MgO (mol%) abundances in peridotite with increased temperature and extents of fusion, assuming conditions for batch melting (after Hanson and Langmuir, 1978). 1. Michael and Bonatti (1985), more refractory peridotite. 2. Prinz et al. (1976), North Atlantic peridotite. 3. Dick and Fisher (1984), average abyssal peridotite. 4. Michael and Bonatti (1985), less refractory peridotite. 5. St. Paul's rocks. 6. Tinaquillo peridotite. 7. Pyrolites.

distribution coefficients for several magmaphilic elements. Despite the aforementioned problems, which are inherent in this type of modeling, the calculations indicate that the Galicia margin peridotite has been melted and depleted by about 7%, a lesser extent than other abyssal peridotites. These calculations are consistent with other estimates of the extent of depletion of the Galicia margin peridotite.

Comparison with Other Peridotites

The preceding discussion suggests that although the Galicia margin peridotites are, on one hand, roughly similar to other

Table 8. Estimated percent melt (or percent depletion) from various peridotites based on batch-melting calculations for Na, Ti, Al, and Ca. The average of the four calculations is given in the final column.

	Ti	Na	Al	Ca	Average
Hole 637A	7.9	5.3	8.7	6.6	7.1
North Atlantic (Prinz et al., 1976)	25.2	2.5	10.8	45.2	20.9
Average abyssal (Dick and Fisher, 1984)	43.0	39.4	25.0	19.0	31.8
Tinaquillo (Jaques and Green, 1980)	6.3	2.5	3.2	1.2	3.3
Zabargad (Bonatti et al., 1986)	1.2	0.3	1.2	0.6	0.8

abyssal peridotites, they appear to have experienced less depletion by partial melting. Therefore, it seems useful to briefly compare the Galicia margin peridotites with other occurrences of ultramafic rocks, including continental peridotites (Ronda peridotite in Spain, Lers in the Pyrenees, and Beni Bouchera in Morocco), as well as other ocean margin peridotites. For other comparative work, see Girardeau et al. (this volume).

The Galicia margin peridotites are dissimilar in composition and lithology to Lers (C. A. Evans, unpubl. data), Ronda (Obata, 1980), and Beni Bouchera (Kornprobst, 1969). For example, no mafic segregations or high-pressure phases (garnet) are found. Important differences in mineral composition between the Galicia margin and continental peridotites are also observed. Figures 8 and 9 display compositional fields for clinopyroxene in continental and abyssal peridotites. Figure 8 shows the Na and Ti abundances in clinopyroxene: clinopyroxene from continental peridotites display a weak positive correlation and are more enriched in both Na and Ti than the Galicia margin samples. A similar positive correlation is seen in Al and Ti concentrations in clinopyroxene from continental peridotites (Fig. 9).

On the other hand, the Na and Cr abundances in clinopyroxene in the Galicia margin peridotites (but *not* the continental peridotites) display a strong correlation (Fig. 7). The high Na abundance in the clinopyroxene from the Galicia margin peridotites led Boillot et al. (1980) to suggest that the peridotite is similar to subcontinental peridotites, based on a Cr-Na diagram constructed for clinopyroxene from upper mantle peridotites in a variety of occurrences (Kornprobst et al., 1981). The Na-Cr coherence in clinopyroxene reflects the partitioning of Na, Al, and Cr between spinel and the pyroxenes, and it may be related to the pressure of pyroxene crystallization (higher pressure would favor a jadeite component in the clinopyroxene). However, Figure 7 shows that the Galicia margin peridotite has lower Na and a different Na-Cr trend than Ronda, Lers, and Beni Bouchera. Abyssal peridotites have clinopyroxene with much lower abundances of Na than the Galicia margin peridotite and no Na-Cr correlation. However, clinopyroxene from the Tinaquillo peridotite also displays a Na-Cr correlation and is correlated with amphibole formation and the presence of plagioclase in the peridotite (M. Seyler, pers. comm., 1986). This is not the case for the Galicia margin samples; mineral assemblages seem to have no correlation with the clinopyroxene composition, with the possible exception of TiO₂ concentration. Thus, the Galicia margin peridotites fall in a field between other abyssal peridotites and subcontinental peridotites. It is suggested that any partial melting will rapidly deplete the clinopyroxene from a fertile peridotite in Na, and any existing Na-Cr correlation will be destroyed. The high Na abundance in clinopyroxene in the Galicia margin peridotites (with respect to other abyssal peridotites) and the Na-Cr correlation are consistent with our interpretation that the Galicia margin peridotite has not participated in substantial partial melting and oceanic basalt formation.

Peridotites from analogous settings at ocean/continental boundaries have been sampled (Red Sea; southwest of Australia). Bonatti et al. (1985) described the Zabargad peridotite in the Red Sea as uplifted upper mantle related to the rifting of the Red Sea. The Zabargad peridotite has a relatively fertile composition and was emplaced at crustal levels prior to basalt production in the Red Sea (Bonatti et al., 1985). Ultramafic blocks were recovered at the edge of the southwest margin of the Australian continent (Nicholls et al., 1981). Again, mineral compositions displayed in Figures 5–9 indicate that these two peridotite bodies are compositionally similar to the Galicia margin peridotite and are likewise less depleted than other abyssal peridotites.

Similar peridotite compositions can also be found in ophiolites that are associated with early rifting events. The Orthris ophiolite is described as an ophiolite formed during the beginning of continental rifting (Menzies and Allen, 1974). The ultramafic rocks from the ophiolite include fertile lherzolite that is compositionally similar to the Galicia margin peridotite (Menzies and Allen, 1974). Based on studies from ophiolites, Boudier and Nicolas (1985) have predicted that the peridotite subtype associated with an incipient ridge or at a very slow-spreading ocean ridge would be lherzolitic. The relatively cooler thermal regime would result in a lesser extent of partial melting. Thus, peridotite (if exposed), would contain more clinopyroxene and have higher abundances of the magmaphilic elements. The undepleted composition of the Galicia margin peridotite, which is also exposed at the edge of a rifted continental margin, is consistent with this hypothesis.

SUMMARY

In summary, the peridotite recovered from the Galicia margin has less depleted compositions than other abyssal peridotites and, in particular, has higher abundances of the magmaphilic elements than other samples of peridotite from the North Atlantic basin. The relatively undepleted nature of the Galicia peridotite may be related to its location at the edge of the ocean basin, at the boundary between oceanic and continental crust. We suggest that it is transitional upper mantle material that was emplaced at crustal levels and exposed on the seafloor prior to the establishment of seafloor spreading. Therefore, it has not participated in extensive partial melting to produce oceanic basalts, although it appears to have been depleted by small amounts of melting (less than 10%). The peridotite was probably uplifted beneath thinned continental crust during the rifting of the continent and last equilibrated at relatively high temperatures (970°–1100°C) and low pressures (less than 9 kbar). However, either the uplift of the peridotite was relatively slow or it started from a shallow and relatively cool region in the mantle; it was not sufficiently hot to rise much above the peridotite solidus and begin extensive partial melting. This thermal constraint is consistent with expected conditions during rifting and incipient seafloor spreading.

ACKNOWLEDGMENTS

We would like to thank the following people for their assistance. E. Bonatti, M. Seyler, S. Bloomer, and E. Wright reviewed the manuscript and provided thoughtful comments and discussion. R. Glynn helped with the manuscript preparation.

REFERENCES

- Bertrand, P., and Mercier, J. C., 1985. The mutual solubility of coexisting ortho- and clinopyroxene: toward an absolute geothermometer for the natural system? *Earth Planet. Sci. Lett.*, 76:109–122.
- Boillot, G., Grimaud, S., Mauffret, A., Mougnot, D., Kornprobst, J., Mergoïl-Daniel, J., and Torrent, G., 1980. Ocean-continent boundary off the Iberian margin: a serpentine diapir west of the Galicia Bank. *Earth Planet. Sci. Lett.*, 48:23–34.
- Bonatti, E., 1976. Serpentine protrusions in the oceanic crust. *Earth Planet. Sci. Lett.*, 32:107–113.
- , 1978. Vertical tectonism in oceanic fracture zones. *Earth Planet. Sci. Lett.*, 37:369–379.
- Bonatti, E., Emiliani, C., Ferrara, G., Honnorez, J., and Rydell, H., 1974. Ultramafic-carbonate breccias from the equatorial Mid-Atlantic Ridge. *Mar. Geol.*, 16:83–102.
- Bonatti, E., Hamlyn, P., and Ottonello, G., 1981. Upper mantle beneath a young oceanic rift: peridotites from the island of Zabargad (Red Sea). *Geology*, 9:474–479.
- Bonatti, E., Ottonello, G., and Hamlyn, P., 1986. Peridotites from the island of Zabargad (St. Jolin), Red Sea: petrology and geochemistry. *J. Geophys. Res.*, 91:599–631.
- Boudier, F., and Nicolas, A., 1985. Harzburgite and lherzolite subtypes in ophiolitic and oceanic environments. *Earth Planet. Sci. Lett.*, 76:84–92.
- Dick, H.J.B., and Bullen, T., 1984. Chromium spinel as a petrogenetic indicator in abyssal and alpine-type peridotites and spatially associated lavas. *Contrib. Mineral. Petrol.*, 86:54–76.
- Dick, H.J.B., and Fisher, R. L., 1984. Mineralogic studies of the residues of mantle melting abyssal and alpine-type peridotites. In Kornprobst, J. (Ed.), *Kimberlites II: The Mantle and Crust-Mantle Relationships*: Amsterdam (Elsevier), 295–308.
- Gast, P. W., 1968. Trace element fractionation and the origin of tholeiitic and alkaline magma types. *Geochim. Cosmochim. Acta*, 32:1057.
- Green, D. H., and Hibberson, W. O., 1970. The instability of plagioclase in peridotites at high pressure. *Lithos*, 3:209–221.
- Green, D. H., Hibberson, W. O., and Jaques, A. L., 1979. Petrogenesis of mid-ocean ridge basalts. In McElhinney, W. (Ed.), *The Earth, Its Origin, Structure and Evolution*: New York (Academic Press), 265–295.
- Hamlyn, P., and Bonatti, E., 1980. Petrology of mantle-derived ultramafics from the Owen Fracture zone, Northwest Indian Ocean: implications for the nature of the oceanic upper mantle. *Earth Planet. Sci. Lett.*, 48:6.
- Hanson, G., and Langmuir, C. H., 1978. Modelling of major elements in mantle-melt systems using trace element approaches. *Geochim. Cosmochim. Acta*, 42:725–741.
- Irving, A. J., 1978. A review of experimental studies of crystal-liquid trace element partitioning. *Geochim. Cosmochim. Acta*, 42:743–770.
- Jagoutz, E., Palme, H., Badenhansen, H., Blum, K., Cendales, M., Dreibus, G., Spettel, B., Lorenz, V., and Wanke, H., 1979. The abundances of major, minor and trace elements in the earth's mantle as derived from primitive ultrabasic nodules. *Geochim. Cosmochim. Acta Suppl.*, 11:2031–2050.
- Jaques, A. L., and Green, D. H., 1980. Anhydrous melting of peridotite at 0–15 kb pressure and the genesis of tholeiitic basalts. *Contrib. Mineral. Petrol.*, 73:287–310.
- Kornprobst, J., 1969. Le massif ultrabasique des Beni Bouchera: étude des péridotites de haute température et de haute pression, qui leur sont associées. *Contrib. Mineral. Petrol.*, 23:283–322.
- Kornprobst, J., Ohnenstetter, P., and Ohnenstetter, M., 1981. Na and Cr contents in clinopyroxene from peridotites: a possible discriminant between "subcontinental" and "suboceanic" mantle. *Earth Planet. Sci. Lett.*, 53:241–254.
- Maaloe, S., and Aoki, K., 1977. The major element composition of the upper mantle estimated from the composition of lherzolites. *Contrib. Mineral. Petrol.*, 63:161–173.
- Menzies, M., and Allen, C., 1974. Plagioclase lherzolite-residual mantle relationships within two eastern Mediterranean ophiolites. *Contrib. Mineral. Petrol.*, 45:197–213.
- Michael, P., and Bonatti, E., 1985. Peridotite composition from the North Atlantic: regional and tectonic variations and implications for partial melting. *Earth Planet. Sci. Lett.*, 73:91–104.
- Mysen, B., and Kushiro, I., 1977. Compositional variations of coexisting phases with degree of melting of peridotite in the upper mantle. *Am. Mineral.*, 62:843–865.
- Nicholls, I., Ferguson, J., Jones, H., Marks, G., and Mutter, J., 1981. Ultramafic blocks from the ocean floor southwest of Australia. *Earth Planet. Sci. Lett.*, 56:362–374.
- Obata, M., 1980. The Ronda peridotite. *J. Petrol.*, 19:340–370.
- Presnall, D. C., Dixon, J. R., O'Donnell, T. H., and Dixon, S. A., 1979. Generation of mid-ocean ridge tholeiites. *J. Petrol.*, 20:3–35.

Prinz, M., Keil, K., Green, J., Reid, A., Bonatti, E., and Honnorez, J., 1976. Ultramafic and mafic dredge samples from the equatorial Mid-Atlantic Ridge and fracture zones. *J. Geophys. Res.*, 81:4087-4103.

Ringwood, A. E., 1979. *Origin of the Earth and Moon*: New York (Springer-Verlag).

Shipboard Scientific Party, 1987. Site 637. In Boillot, G., Winterer, E. L., et al., *Proc. ODP, Init. Repts.*, 103: College Station, TX (Ocean Drilling Program), 123-219.

Sinton, J. M., 1979. Petrology of alpine-type peridotites from Site 395, DSDP Leg 45. In Melson, W. G., Rabinowitz, P. D., et al., *Init. Repts. DSDP*, 45: Washington (U.S. Govt. Printing Office), 595-601.

Date of initial receipt: 6 January 1987

Date of acceptance: 25 May 1987

Ms 103B-138